

Functional Finishing of Textile using Manganese Doped Zinc Oxide based Coatings Obtained by Sol-gel Method

MARIANA (BUSILA) IBANESCU¹, VIORICA MUSAT^{1*}, TORSTEN TEXTOR², BORIS MAHLTIG³

¹ "Dunărea de Jos" University of Galați, Centre of Nanostructures and Functional Materials-CNMF, 111 Domnească Str., 800201, Galați, Romania

² Deutsches Textilforschungszentrum Nord-West GmbH, DTNW GmbH, Adlerstr. 1, 47798 Krefeld, Germany and CENIDE, Center for Nanointegration Duisburg-Essen

³ University of Applied Sciences, Faculty of Textile and Clothing Technology, Webschulstr. 31, 41065 Mönchengladbach, Germany

This paper reports photocatalytic activity of ZnO and Mn-doped ZnO nanoparticles obtained by modified sol-gel method. Structural and morphological properties of nanoparticles were characterized by X-ray diffraction (XRD) and scanning electron microscopy (SEM); the average crystallite size of ZnO and Mn-doped ZnO was 14.7 and 4.2 nm, respectively. These oxides were used as efficient photocatalysts which can effectively degrade organic contaminants with UV light irradiation. Due to the ability to be photoactive these nanoparticles can induce antimicrobial activity. The photocatalytic activity of nanoparticles was investigated as coatings on textile fabrics. The coating process was carried out on pure cotton (100%) and cotton/PES 50/50% using the pad-dry-cure method. The investigation of the photocatalytic activity was based on the degradation of the methylene blue (MB) in the presence of ZnO and Mn: ZnO nanoparticles, in powder or applied to the textile fabrics, under UV light irradiation ($\lambda = 210$ nm). With the increasing of the Mn doping, the optical band gap increases indicating enhanced photocatalytic activity of nanoparticles.

Keywords: ZnO nanoparticles, Mn doping, band gap, photocatalysis

In the recent years, textile materials were functionalized with different coatings. Functional finishing of textiles, clothing and textiles for footwear is one approach to the realization of highly active surfaces to have UV-blocking, self-cleaning properties. Due to the ability to be photoactive, ZnO nanoparticles can induce antimicrobial activity once coated on the textiles [1].

There are a few methods in the literature that describe the coating of fabrics with ZnO nanoparticles, for example, the pad-dry-cure method, plasma radiation, thermal and chemical treatments. [2-5].

Recently, Zinc oxide nanoparticles are widely used in different areas such as photo-catalysis and catalyst, sunscreens, coatings and paints because of its high UV absorption efficiency. In the same time, it shows strong antibacterial activities on a broad spectrum of bacteria [6-17].

ZnO is a n-type II-VI semiconductor with direct and wide band gap of 3.44 eV at low temperature and 3.37 eV at room temperature, high efficient UV emission resulting from a large excitation binding energy, 60 MeV at room temperature, high specific area, fine particle size, quantum confinement properties, non-toxic, inexpensive, high resistant to deoxidation [18].

Specific surface area and surface defects play an important role in the photocatalytic activities of metal oxide. The reason is that, doping of metal oxide with metal and/or transition metals increases the surface defects [19]. In addition it affects the optical and electronic properties [20] and can shift the optical absorption towards the visible region.

In this paper, we present improved photocatalytic activities of ZnO doped with manganese ion (Mn^{2+}). UV light was used as source of radiation and methylene blue as test contaminant. The preliminary results presented in

this work show much promise and suggest the need to further explore heterogeneous photocatalysis mechanism.

Experimental part

Preparation of undoped ZnO and Mn-doped ZnO (Mn^{2+} : ZnO)

The preparation procedure was similar to that of Spanhel and consists of two major steps [21]. The first is the suspension of the precursor and the second is the hydrolysis of the precursor to obtain the zinc oxide nanoparticles. Zinc acetate dihydrate ($ZnAc)_2 \cdot 2H_2O$ (99%-Sigma Aldrich), manganese (II) sulfate monohydrate ($MnSO_4 \cdot xH_2O$ -0,1; 5; 15 at%,) (99%-Sigma Aldrich, and isopropanol (99,8%-Fluka) were used to prepare the precursor and lithium hydroxide (LiOH-Merk) was used to hydrolyze the precursor.

For synthesizing the catalyst, 0.035M of $(ZnAc)_2 \cdot 2H_2O$ in 500 mL 2-propanol was mixed with different concentrations of manganese (II) sulfate by reflux heating 82°C (boiling point) for three hours. An amount of 0.035M lithium hydroxide was dissolved in 500 mL isopropanol at room temperature by vigorous magnetic stirring. The new colorless solution was cooled down to 0°C before the lithium hydroxide solution was added drop wise under vigorous stirring. The ZnO sol was stored at $\leq 4^\circ C$ for 24 h.

For separating Mn-doped ZnO nanoparticles and to remove the residual products, high-speed centrifugation 4000 rpm/20 min was used followed by several alcoholic washes. After the washing it is dried in an oven at 60 °C to obtain powder. This powder is weighed and finally redispersed in alcohol to be ready for application to the textile.

Coating of Nanoparticles on Textile Substrate

The coating experiments were carried out using plain-weaved fabrics made of scoured and bleached cotton

* email: viorica.musat@ugal.ro; Tel: 0757070613

(100%), with a mass per unit area of 250g/m², and blended fabrics made of polyester/cotton (50/50%) with a mass per unit area of 182 g/m². Both materials were standard test materials supplied by WFK, Germany.

Appropriate finishing solutions have been found as: Zinc oxide nanoparticles dispersion (100mL), containing 0.3g ZnO and Mn 0.1, 5, 15at %/ZnO, GPTMS sol (5 mL), TEOS (5 mL) and 30mL 0.01N HCl were mixed together for 2 h by magnetic stirring.

The organic-inorganic sol was applied to the fabrics by a pad-dry-cure- method. The coating was carried out by a padding process with a laboratory padder equipped with roles (Mathis, Switzerland). The nip-pressure was adjusted to a value guaranteeing a wet pick up of 100%; the role speed was 4m/min. After padding, the samples were dried in a labcoater (Mathis, Switzerland) at 130°C for 30 min before they were washed to remove residual by-products.

Characterization of Nanoparticles

The crystal structures of the product were identified by X-ray diffraction patterns DRON-3 diffractometer system (Burevestnik, USSR) with CoK α radiation, $\lambda = 1.789 \text{ \AA}$.

The crystallite size of the particles was calculated with Debye-Scherrer formula (1):

$$D = \frac{0,94\lambda}{\beta \cos \theta} \quad (1)$$

The value of interplanar distance (d) was calculated with Bragg's equation (2):

$$2d \sin \theta = n\lambda \quad (2)$$

and lattice parameters (3):

$$\frac{1}{d^2} = \frac{4(h^2+hk+k^2)}{3a^2} + \frac{l^2}{c^2} \quad (3)$$

The calculation is based on the measurement of full-width at half-maximum (FWHM) values in the corresponding XRD pattern.

The morphology and the composition of the product were examined by scanning electron microscopy (SEM, type Hitachi S 3400N with tungsten cathode, coated with gold Emitech K500X sputter coater, Oxford X-Max SDD X-ray Energy Dispersive Spectrometer (EDS)

Band gap energy value for ZnO nanoparticles was calculated with formula (4) [22]:

$$E_g = h \frac{c}{\lambda} \quad (4)$$

UV/Vis Absorption measurements for that material are being carried out using a Cary 5E UV-Vis-NIR Spectrophotometer, Varian Deutschland GmbH with integrating sphere.

Photocatalytic measurements

Photocatalytic properties of the samples were investigated by measuring the UV absorption at room temperature using a Cary 5E UV-Vis-NIR Spectrophotometer. The photocatalytic activities of doped and undoped samples were evaluated by measuring photodegradation of Methylene Blue (MB) (20 mg/L added to 40 mL in water) in presence the 0.1g powder of ZnO and Mn (0.1, 5, 15wt%):ZnO nanoparticles, in Petri dish, under ultraviolet illumination (>251nm) for 1hour. The photocatalytic activity of the coated fabrics was tested using coated disks with 8 cm diameter, placed in Petri dish before adding the MB solution.

Results and discussions

Crystal structure of the prepared nanoparticles is presented in XRD patterns (fig. 1). The peaks at $2\theta = 37.52^\circ$, 40.44° , 42.77° were assigned to (100), (002), (101) of ZnO planes, indicating the wurtzite structure. No characteristic peaks of manganese metal or oxides phases were observed by XRD.

Using the Debye-Scherrer equation and the halfwidth of the XRD lines, the average values of crystalline size of the samples were calculated based on the (101) crystal plane.

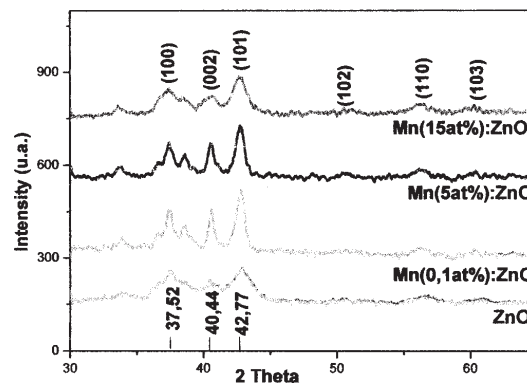


Fig. 1. XRD patterns for ZnO and Mn:ZnO nanoparticles with different concentrations: a) ZnO; b) Mn:ZnO-1; c) Mn: ZnO-2; d) Mn:ZnO-3

The crystalline phases obtained by analysis of the XRD patterns are shown in figure 1 and the structural parameters as main crystallite size (D), interplanar distance (d) and lattice parameters (a and c) were calculated and presented in table 1.

Table 1
XRD STRUCTURAL PARAMETERS FOR ZnO AND DIFFERENT CONCENTRATIONS OF Mn DOPED ZnO NANOPARTICLES

Sample	Mn (at%)	D (nm)
ZnO	-	14.7
Mn:ZnO-1	0.1	12.9
Mn:ZnO-2	5	11.8
Mn:ZnO-3	15	4.2

In figure 2, the SEM images on the surfaces of the cotton 100% (fig 2a, c, e, g) and cotton/polyester 50/50% (fig 2 b, d, f, h) fabrics, uncoated and coated with ZnO and Mn-doped ZnO nanoparticles are shown.

The crystalline size of photocatalyst decreased with increasing percentage of Mn. It may be due to the doping of Mn in ZnO that can control the crystal size, as observed for other transition metals such as Co [23] and Cr [24].

Small nanoparticles and agglomerates of nanoparticles dispersed on the fiber surface in both cases can be observed. Small amount of nanoparticles can be observed on the surface of cotton fibers and cotton-polyester blend (fig. 2b, 2f) as compared with that observed on the surface of the same fiber where the dopant amount increases. The particle size plays an important role in determining their adhesion to the fiber, it is reasonable to expect that the largest particle agglomerates will be easily removed from the fiber surface, while the smaller particles will penetrate deeper and adhere strongly into the fabric matrix. SEM images confirm that the large agglomerated nanoparticles also remain on the textile surface after washing.

For the calculation of the band gap value, optical absorption spectra were used. When a semiconductor

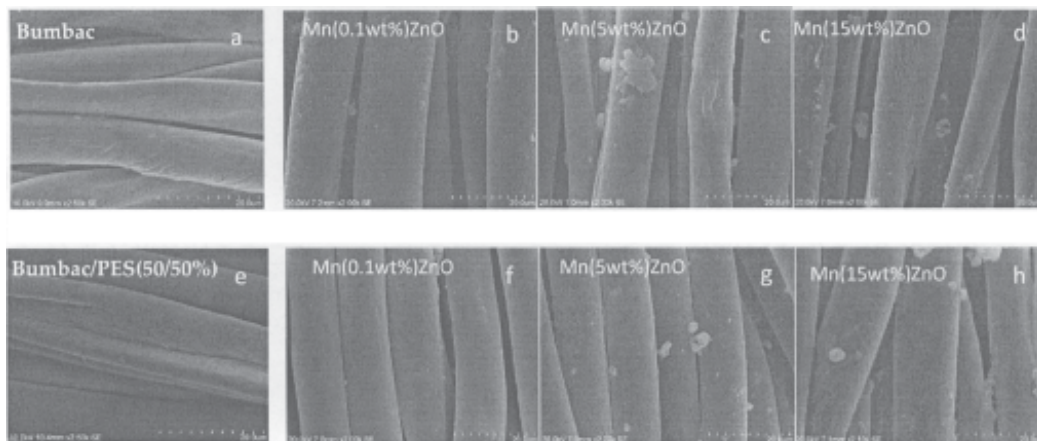


Fig. 2. SEM micrographs on the surfaces of the cotton 100% (a, b, c, d) and cotton/polyester 50/50% (e, f, g, h) fabrics, uncoated (a-e) and coated with 0.1% Mn-doped ZnO (b-f), 5% Mn-doped ZnO (c-g) and 15% Ag-doped ZnO (d-h) nanoparticles

absorbs photons of energy larger than the gap of the semiconductor, an electron is transferred from the valence band to the conduction band, an abrupt increase in the absorptivity of the material occurs to the wavelength corresponding to the band gap energy.

The UV-Vis optical absorption spectra of ZnO and as-prepared Mn:ZnO nanoparticles are presented in figure 3. The optical absorption edge presents a blue shift to the region of higher photon energy, when Mn concentration increases. This blue shift confirms preventing the recombination of photoexcited electrons and holes induced by Mn-acceptor doping and so the increase in carrier concentration.

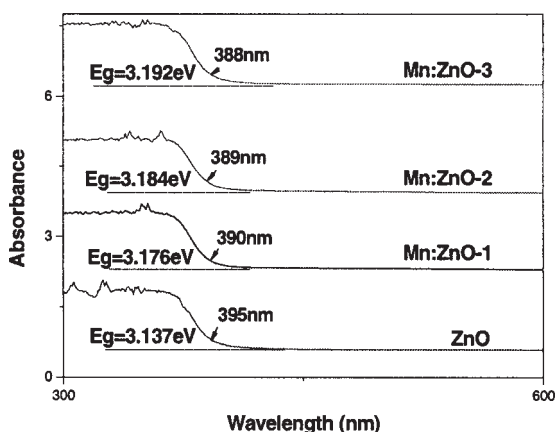


Fig. 3. UV-VIS absorption spectra of ZnO and Mn:ZnO nanoparticles

The values of optical band gap (E_g) show a widening up to 3.192 eV as compared to the values of 3.137 eV obtained for ZnO nanoparticles when the Mn – doping concentration increases up to 15at%. In general, according to Burstein–Moss effect, the blue shift of the absorption onset is associated with the increase of the carrier concentration blocking the lowest states in the conduction band [25].

The photocatalytic properties were studied using ZnO and different concentrations of Mn doped ZnO nanoparticles on degradation of methylene blue (MB). Extent of photocatalytic degradation was determined by the reduction in absorbance of the solution. As a result of the reaction between ZnO nanoparticles (through the reactive oxygen species on its surface) and MB dye, the rate of decolorisation was changed as the increased the dopant concentration of ZnO nanoparticles.

UV-Vis absorption spectra of the residual blanch solution of methylene blue after 60 min UV-irradiation in normal laboratory environment in presence of ZnO nanoparticles and Mn (different concentration):ZnO nanoparticles, as-prepared powders or deposited on textile fabrics, are shown in figures 4 - 6 and 8, respectively.

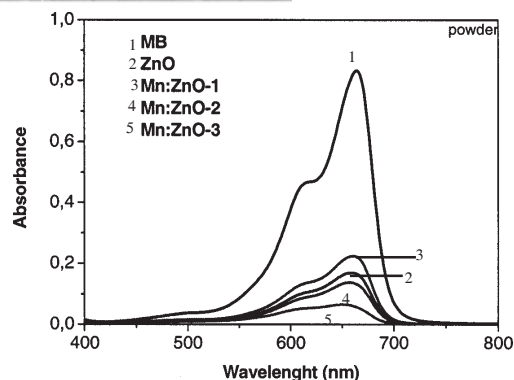


Fig. 4. UV-Vis absorption spectra of methylene blue in presence of different concentrations of Mn doped ZnO nanoparticles (powder) after UV-irradiation

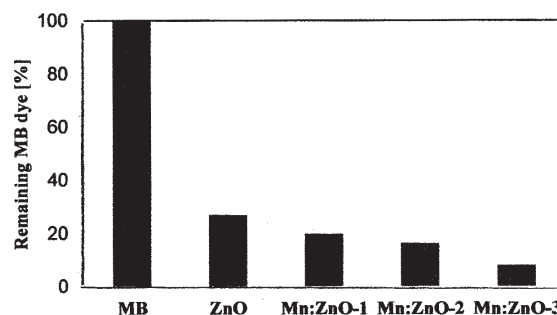


Fig. 5. Photocatalytic degradation of MB in the presence ZnO and Mn:ZnO nanoparticles (different concentrations of Mn doping)

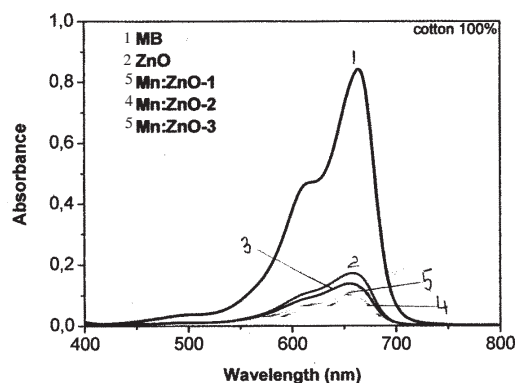


Fig. 6. UV-Vis absorption spectra of methylene blue in the presence of different concentrations of Mn doped ZnO nanoparticles (applied on cotton 100%) after UV-irradiation

After 1 hour UV irradiation of MB solutions, in the presence of nanoparticles, occurs a high photodegradation that increases from 73% for the ZnO, 80% for Mn: ZnO-1, 83% for Mn: ZnO, 2 to 91% for Mn: ZnO-3.

The photocatalytic activity under UV irradiation of fabrics coated with ZnO and Mn:ZnO nanoparticles (fig. 6-8) also

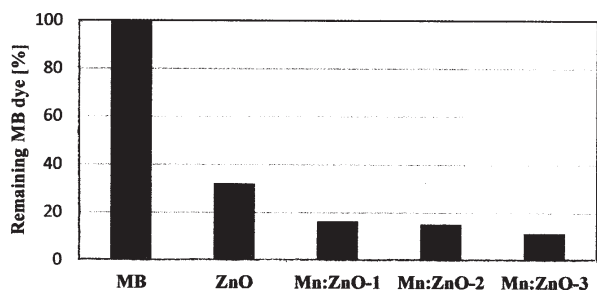


Fig. 7. Photocatalytic degradation of MB in the presence ZnO and Mn:ZnO nanoparticles (different concentrations of Mn doping) applied on cotton 100%; ZnO; Mn:ZnO- 1 (0.1at%); Mn:ZnO- 2 (5at%); Mn:ZnO- 3 (15at%)

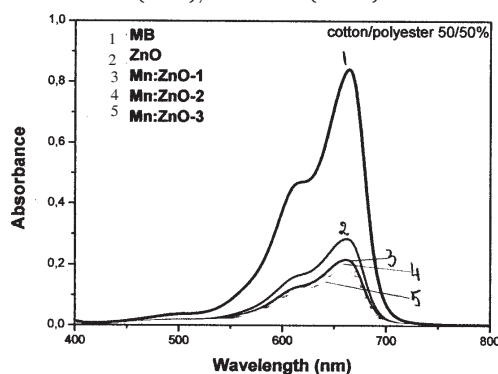


Fig. 8. UV-Vis absorption spectra of methylene blue in the presence of different concentrations of Mn doped ZnO nanoparticles (applied on cotton/PES 50/50%) after UV-irradiation.

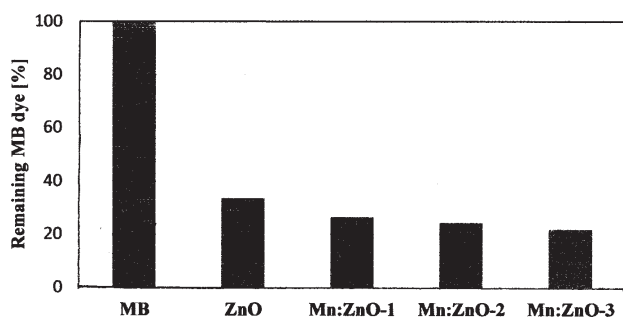


Fig. 9 Photocatalytic degradation of MB in the presence of ZnO and Mn:ZnO nanoparticles (different concentrations of Mn doping) applied on cotton-polyester 50/50%; ZnO; Mn:ZnO- 1 (0.1at%); Mn:ZnO- 2 (5at%); Mn:ZnO- 3 (15at%)

shows decolorization increase when the Mn - doping concentration increases from 0.1 to 5 and 15 at% Mn due to increased photocatalytic activities, but with lower rate of decolorisation. The same observation can be made in figure 8 when the fabric was changed to cotton/polyester (50/50%).

In figure 7 it can be seen that the photodegradation of MB solutions in the presence of the nanoparticles deposited on cotton, for the ZnO increased from 69% to 84% for Mn: ZnO-1, 83% for Mn: ZnO-2 and to 89% for Mn: ZnO-3.

It is observed that the samples tested showed good photocatalytic activity for nanoparticles deposited on cotton-polyester, with an increase from 67% for ZnO to 73% for Mn: ZnO-1, 76% for Mn: ZnO-2 and until 78% for Mn: ZnO-3.

Here, was assumed that upon illumination with UV light, Mn:ZnO generates electron-hole pair at the tail states of conduction band and valence band, respectively. The generated electron transfers to the adsorbed MB molecule on the particle surface, because it is a cationic dye. The excited electron from the photocatalyst conduction band

enters into the molecular structure of MB and disrupts its conjugated system which then leads to the complete decomposition of MB. The hole at the valence band generates OH^\bullet via reaction with water or OH^- ; might be used for oxidation of other organic compounds. This clearly demonstrates that ZnO doped with manganese (Mn:ZnO) can be used as a potential photocatalyst, which can operate at visible light and it is evident that doping of ZnO with transition metals like Mn enhances photocatalytic activity of ZnO, and hence Mn:ZnO is capable of degrading MB and other organic dyes even under the UV light irradiation [26].

Conclusions

ZnO and Mn:ZnO nanoparticles were prepared using a solvothermal process at a temperature below 90°C. ZnO and Mn:ZnO nanoparticles sol has long stability for further processing.

The XRD measurement confirms that all, undoped and Mn-doped ZnO, nanoparticles consist of Wurtzite-type nanocrystallites with different crystalline orientations, (101) being the dominating peak. The Mn atoms substitute Zn sites in the lattice without changing the wurtzite structure. No secondary phases were observed.

Nanoparticles - based coatings on the textile support were obtained by the pad-dry-cure method and drying at moderate temperatures in ventilated oven is appropriate (130°C for 30 min).

The photocatalytic activity of undoped and Mn-doped ZnO nanoparticles applied on cotton shown decoloration of a Methylene Blue (MB) solution, 1h under UV light, as a result of the reaction between the reactive oxygen species from the surface of ZnO nanoparticles and MB dye. The rate of decolorization changed when the Mn:ZnO nanoparticles sample changed. Higher Mn -doping concentration, lower intensity of absorption in visible region, due to higher photocatalytic activities. Very encouraging results for photocatalytical properties impose new research regarding antimicrobial activity of Mn doped ZnO nanoparticles.

Acknowledgements: The work of Mariana (Busila) Ibanescu was supported by Project SOP HRD – TOP ACADEMIC 78622

References

- LAMB R, ZHANG H, JONES A and Postle R Proc. 83rd TIWC, Shanghai, China, 2004, p. 682
- LI, J.H., HONG, R.Y., LI, M.Y., ZI, H.Z., ZHENG, Y., J. Ding, Organ. Coat. **64**, 2009, p. 504
- ZOHDI, M.H., KAREM, H., EL-NAGGAR, A.M., HASSAN, M.S., J. Appl. Polym. Sci. **89**, 2002, p. 2604
- VIGNESHWARAN, N., KUMAR, S., KATHE, A.A., VARADARAJAN, P.V., PRASAD, V., Nanotechnology **17**, 2006, p.5087–5095.
- PERELSHEIN, I., APPLEROT, G., PERKAS, N., WEHRSCHEITZ-SIGL, E., HASMANN, A., GUEBITZ, G.M., GEDANKEN, A., ACS Appl. Mater. Inter. **1**, 2009, p. 361
- PAN, Z.W., DAI, Z.R., WANG, Z.L., Science, **291**, 2001, p. 1947–1949.
- ARNOLD, M.S., AVOURIS, P., PAN, Z.W., WANG, Z.L., J.Phys. Chem. B, **107**, 2003, p.659–663.
- XIONG, M., GU, G., YOU, B., WU, L., J.Appl.Pol. Sci., **90**, 2003, p.1923–1931.
- BEHNAJADY, M.A., MODIRSHAHLA, N., HAMZAVI, R., J.Hazard. Mat., **133**, 2006, p. 226–232.
- LI, Y.Q., FU, S.Y.Y., MAI, M., Polymer **47**, 2006, p. 2127–2132.
- TANG, E., CHENG, G., MA, X., PANG, X., ZHAO, Q., Appl. Surf. Sci., **252**, 2006, p. 5227–5232.
- WANG, Z.L., J.Phys. Cond. Mat., **16**, 2004, p. 829–858.
- WANG, Z.L., J.Phys.Cond. Mat., **7** (6), 2004, p.26–33.

14. WANG, Z.L., Appl. Phys. A, **88**, 2007, p. 7–15.
15. VIGNESHWARAN, N., KUMAR, S., KATHE, A.A., VARADARAJAN, P.V., PRASAD, V., Nanotechnology **17**, 2006, p.5087–5095.
16. BECHERI, A., DURR, M., NOSTRO, P.L., BAGLIONI, P., J. Nanop. Res., **10**, 2007, p. 679–689.
17. XU, T., XIE, C.S., Progress in Organic Coatings **46**, 2003, p. 297–301.
18. MAKINO, T., CHIA, C.H., TUAN, N.T., SUN, H.D., SEGAWA, Y., KAWASAKI, M., Appl. Phys. Lett., **77**, 2000, p. 975
19. WANG R., XIN J.H., YANG Y., LIU H., XU L., HU J., Appl. Surf. Sci., **227**, 2004, p.312–317.
20. VANHESUDEN K., WARREN W.L., VOIGT J.A., SEAGER C.H., TALLANT D.R., Appl. Phys. Lett. **67**, 1995, p. 1280–1282.
21. SPANHEL L.; ANDERSON M. A., J. Am. Chem. Soc., **113**, 1991, p. 2826
22. DHARMA J., Perkin Elmer Technical Center; Aniruddha Pisa-Global Application Laboratory Perkin Elmer, Inc. Shelton, CT USA,
23. VOLBERS, N.; ZHOU, H.; KNIES, C.; PFISTERER, D.; SANN, J.; HOFMANN, D. M.; MEYER, B. K., Applied Physics A, **88** (1), 2007, p. 153-5
24. LI, L.; WANG, W.; LIU, H.; LIU, X.; SONG, Q.; REN, S., J.Phys. Chem.C, **113** (19), 2009, p. 8460-4.
- 25.] ZI-QIANG, X., HONG, D., YAN, L., Hang, C., Mat. Sci. Semicon. Proc., **9**, 2006, p.132–135.
26. ULLAH R., DUTTA J, J. Hazard Mater., **156** (1-3), 2008, p. 194–200

Manuscript received: 12.12.2013